Supplemental Figures

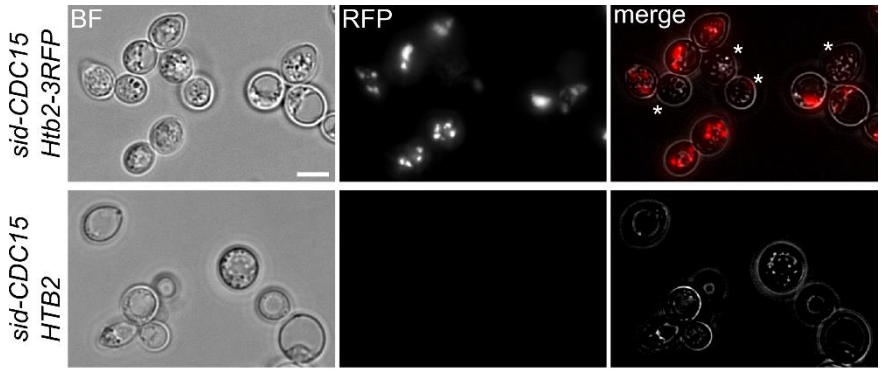

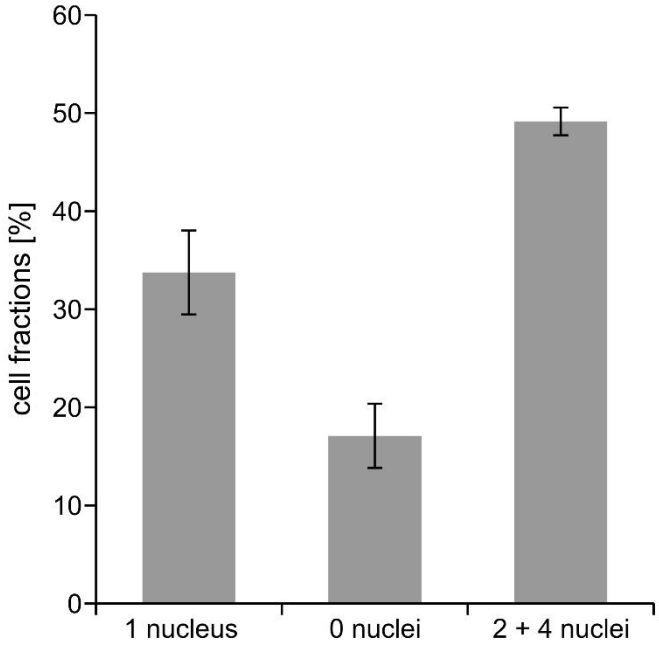

Figure S1 – A considerable fraction of cells loses Htb2-3mCherry signals during sporulation. Strains with *sid-CDC15 HTB2-3mCherry* (YCT1381) and *sid-CDC15* (YCR332) were sporulated in liquid medium containing 1 % potassium acetate. Fluorescence microscopy was performed after 48 h in sporulation medium. Cells that do not show Htb2-3mCherry signal in YCT1381 cells are marked (*) in the merge image. The graph shows quantification of the cell species. The mean of four biological replicates is shown (error bars: S.E.M.; 105 - 510 cells were evaluated for each replicate).

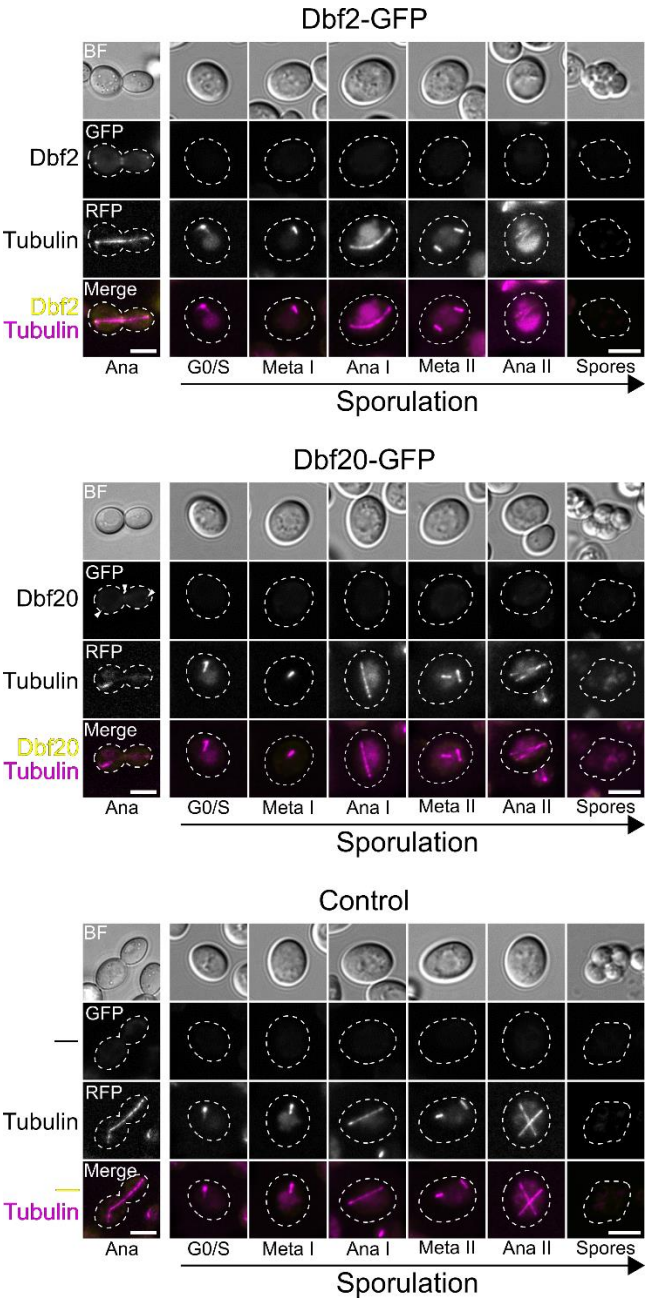

Figure S2 – Live-cell imaging of Dbf2-GFP and Dbf20-GFP localization during sporulation. Strains with an *RFP-TUB1* fusion integrated at the *TRP1* locus and either no further modification (Control; YAL19), *DBF2-GFP* (YAL47) or *DBF20-GFP* (YAL48) were subjected to sporulation conditions and images were taken hourly from 4 h to 9 h. Cells were classified to the different sporulation stages according to spindle and cell morphology. Images of cells in mitotic anaphase are included as reference (left panels). Cell outlines are indicated as broken lines. Scale bars: 5 µm (please note the smaller scale in the mitotic images).

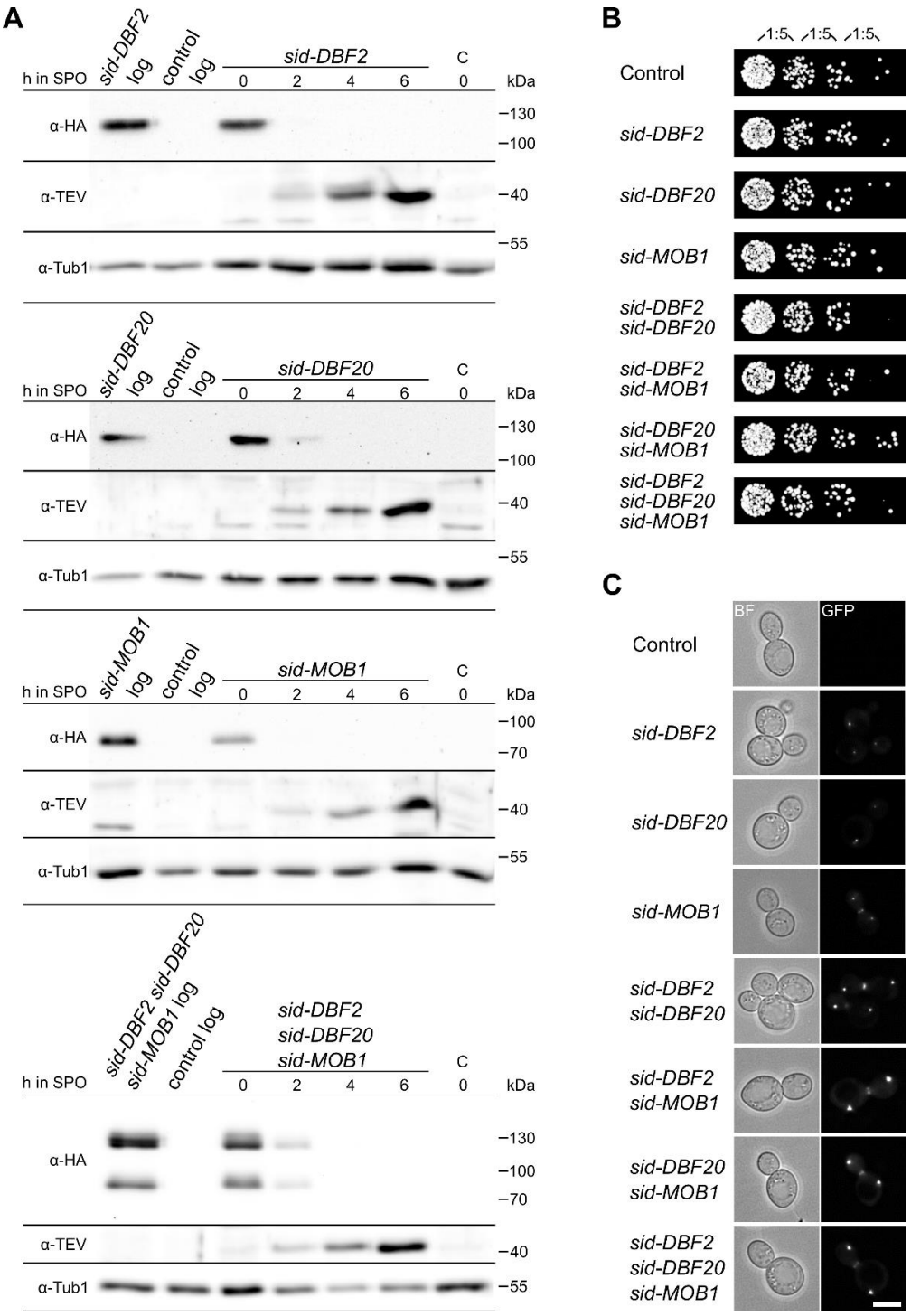

Figure S3 – Sporulation-specific protein depletion and vegetative characterization of *sid-DBF2*, *sid-DBF20* and *sid-MOB1*.

A – Meiotic depletion of Dbf2, Dbf20 and Mob1 separately or in the same strain. Depletion strains for Dbf2↓ (YCR359), Dbf20↓ (YCR344), Mob1↓ (YCR333), and Dbf2↓ Dbf20↓ Mob1↓ (YCR446) were subjected to sporulation in liquid medium with 1 % acetate. Samples were collected hourly from 0 h to 6 h. Additionally, samples from mid-log cultures in YPD were taken. Samples of a strain with only the P_{IME2}-*pTEV*$^{+}$-T_{DIT1} construct (YCR329) collected at 0 h were used as control (C). Fusion proteins were detected by anti-HA antibodies, TEV protease production was monitored by anti-TEV antibody and anti-Tub1 signals served as loading controls.

B – Vegetative growth of strains with different combinations of *sid-DBF2*, *sid-DBF20* and *sid-MOB1*. Serial 1:5 dilutions of indicated mutants (Dbf2↓: YCR359; Dbf20↓: YCR344; Mob1↓: YCR333; Dbf2↓ Dbf20↓: YCR363; Dbf2↓ Mob1↓: YCR447; Dbf20↓ Mob1↓: YCR450; Dbf2↓ Dbf20↓ Mob1↓: YCR446) and the control strain (YCR329) were spotted on YPD plates and images were taken after two days incubation at 30 °C.

C – Mitotic localization of the fusion proteins. Cultures of the same strains as in **B** were grown to mid-log phase in LFM with 2 % glucose and images were taken in brightfield (BF) and GFP channels. Scale bar: 5 µm.

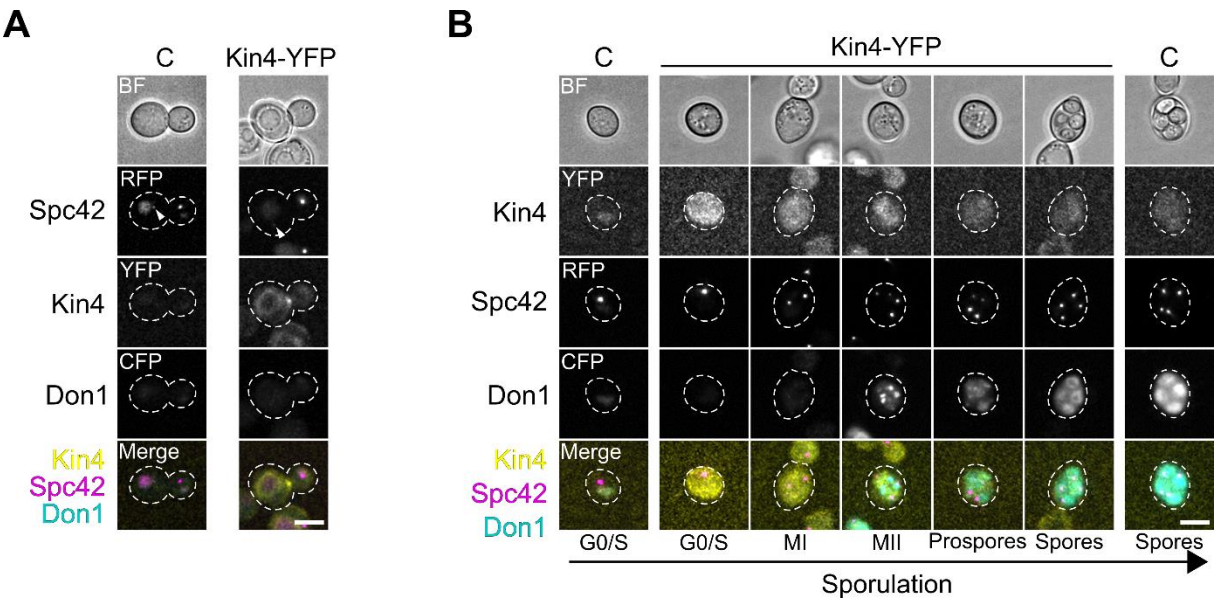

Figure S4 – Localization of Kin4 during mitosis and sporulation.

A – Mitotic localization of Kin4. Kin4-YFP localization was checked in a strain with Spc42-RFP and Don1-CFP fusions (YAA250), a strain without Kin4-YFP served as control (C; YAA249). Cells were grown to mid-log phase in LFM + 2 % glucose and subjected to fluorescence microscopy. Images from brightfield (BF) and the different fluorescence channels are shown together with a color merge of the fluorescence images. Cell outlines are marked as broken lines. Filled triangles point to the younger SPB. Scale bar: 5 µm.

B – Localization of Kin4 during sporulation. Same strains as in **A** were subjected to sporulation conditions and images were taken at 0 h and hourly between 5 h and 10 h after induction of sporulation. Sporulation stages were assigned according to SPB signals of Spc42-RFP and Don1-CFP at the leading edge of the PSMs. For the control, cells in G0/S phase as well as with refractive spores are shown to account for spore wall autofluorescence in the CFP channel. Scale bar: 5 µm.

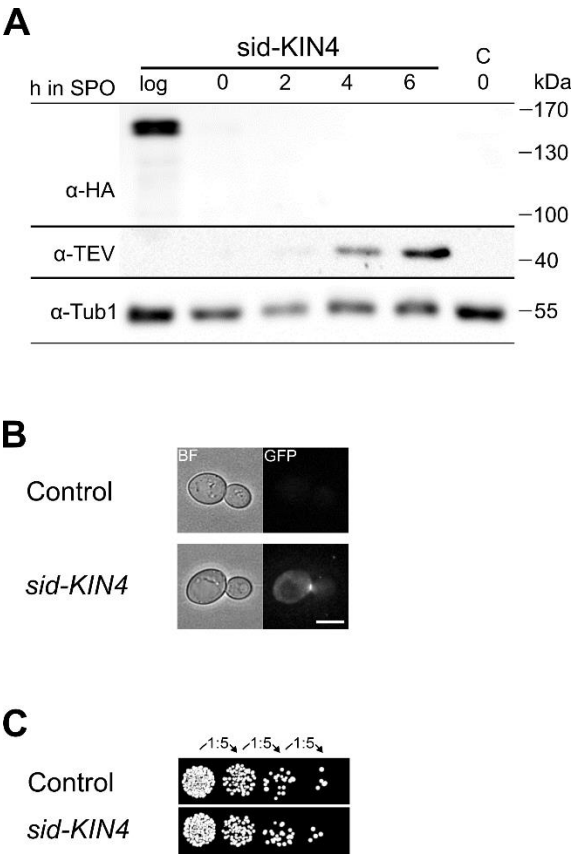

Figure S5 – Sporulation-specific protein depletion and vegetative characterization of the *sid-KIN4* strain.

A – Sporulation-specific depletion of sid-Kin4. Sporulation in liquid 1 % acetate was performed with a sid-Kin4 (YAA215) and a control strain (C; YAA146). Samples were collected at the indicated time points. Anti-HA antibody was used for detection of the fusion protein, anti-TEV antibody allowed observation of $pTEV^{+}$ levels and anti-Tub1 antibody served as loading control.

B – Mitotic localization of sid-Kin4. The strains of **A** were grown to mid-log phase in LFM + 2 % glucose. Images were taken in the brightfield (BF) and GFP channel. Scale bar: 5 µm.

C – Vegetative growth of the *sid-KIN4* strain. Serial 1:5 dilutions of the same strains as in **A** were spotted on YPD solid medium and images were taken after 2 days at 30 °C.

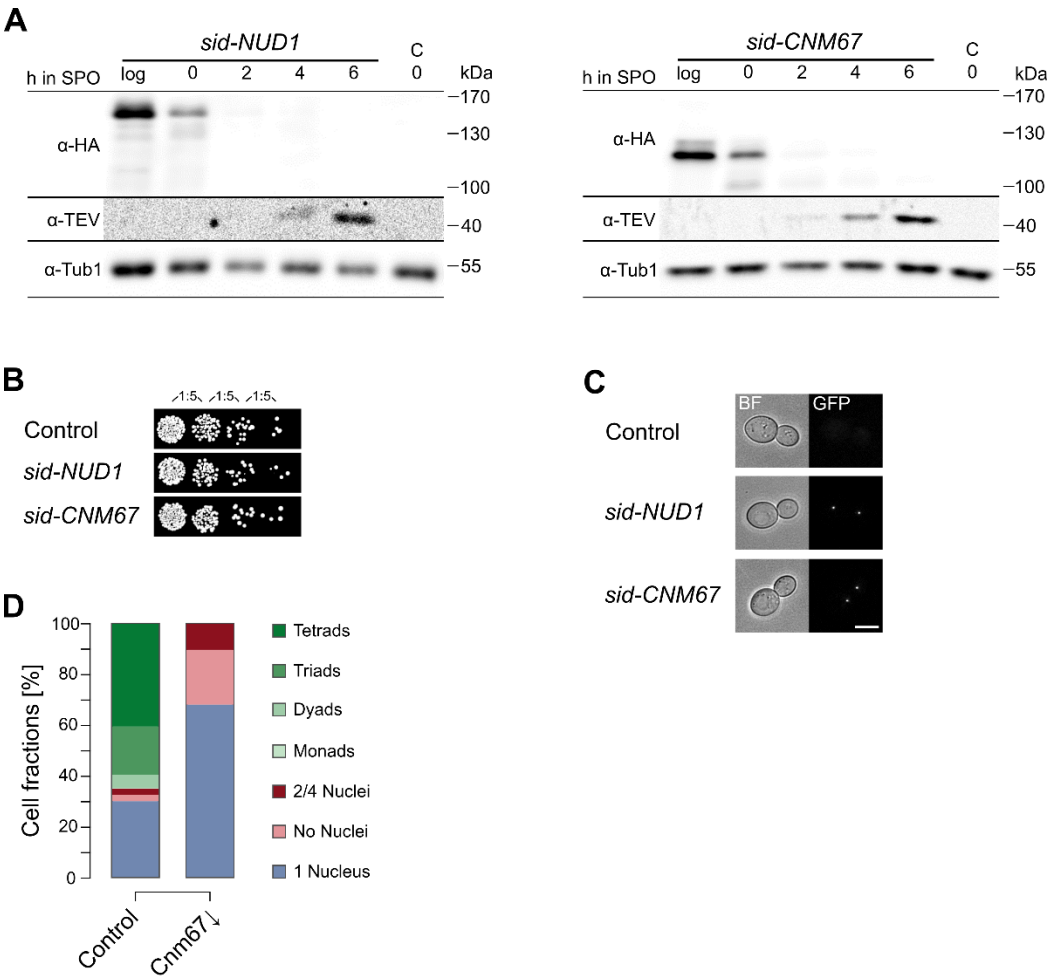

Figure S6 – Sporulation-specific protein depletion, vegetative characterization, and sporulation of the *sid-NUD1* and *sid-CNM67* strains.

A – Sporulation-induced depletion of sid-Nud1 and sid-Cnm67. Depletion mutants of Nud1 (YAA216) and Cnm67 (YAA187) were sporulated together with a control strain (C; YAA146) in liquid 1 % acetate. Samples were collected at the indicated time points. The fusion proteins were detected by anti-HA antibody, pTEV$^+$ production was followed with anti-TEV antibody and anti-Tub1 antibody was used for loading control.

B – Vegetative growth of the *sid-NUD1* and *sid-CNM67* strains. Serial 1:5 dilutions of the strains of **A** were spotted in on solid YPD medium and images were taken after 2 days at 30 °C.

C – Mitotic localization of sid-Nud1 and sid-Cnm67. The same strains as in **A** were grown to mid-log phase in LFM + 2 % glucose and images in brightfield (BF) and GFP channels were taken. Scale bar: 5 µm.

E – Sporulation profiles of the Cnm67↓ mutant strain. A Cnm67↓ (YAA187) and control (C; YAA146) strain were sporulated on solid medium with 1 % acetate. Cells were counted according to cell morphology and number of nuclei. Means of at least 3 biological replicates are shown, between 97 and 488 cells per replicate were counted. Please see Table S1 for statistical evaluations.

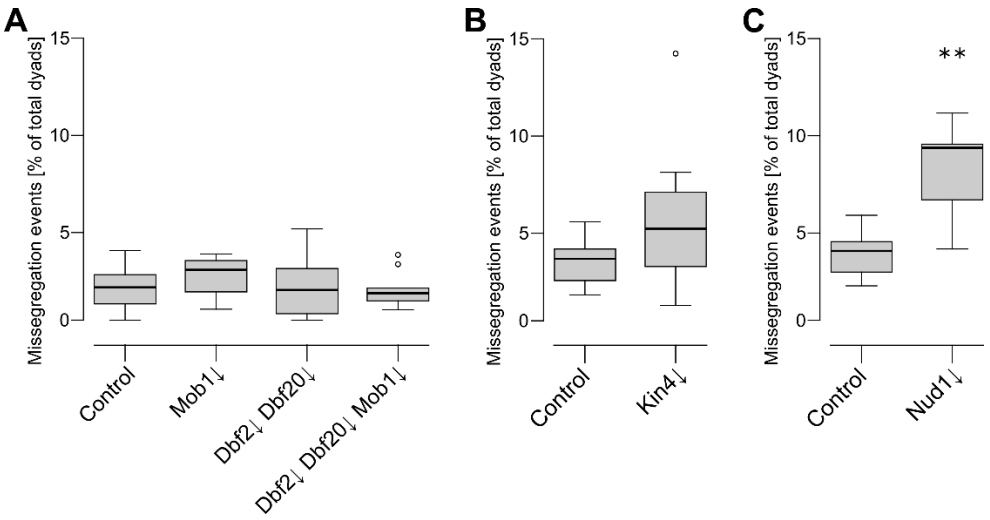

Figure S7 – Chromosome segregation in MEN mutants

A – Chromosome segregation in dyads of the Mob1↓, Dbf2↓ Dbf20↓ and Dbf2↓ Dbf20↓ Mob1↓ strains. The experiments shown in Figure 3B were evaluated with regard to chromosome V missegregation events. Dyads with either one red and one green or both red or green colored spores were classified as faithful segregation events while dyads with one or two spores without or with both fluorophores were counted as missegregation events and fractions of total dyad number was visualized. No statistical significant differences to the control were found by Wilcoxon-Mann-Whitney tests ($n \geq 12$; 88 – 349 cells per replicate).

B – Kin4 depletion does not affect chromosome segregation. Dyads of the same experiment as in Figure 3B were evaluated regarding chromosome segregation defects (two-colored or non-colored spores). Differences to the control were not statistically significant (Wilcoxon-Mann-Whitney test; $n \geq 11$; 119 – 418 cells per replicate).

C – Chromosome segregation defects in the Nud1↓ mutant. Dyads of the same experiment as in Figure 3B were evaluated regarding chromosome segregation defects (two-colored or non-colored spores). Statistical significance of the difference was checked by a Wilcoxon-Mann-Whitney test ($n \geq 8$; **: $p \leq 0.01$; 145 – 358 cells per replicate).

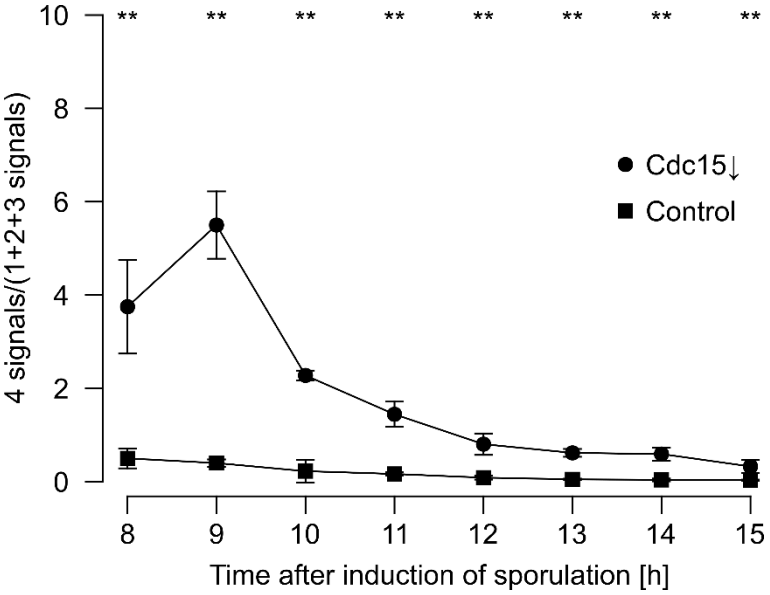

Figure S8 – Cdc15↓ cells show high number of cells with four meiotic plaques. The experiments shown in **Figure 5A** (time points 8 to 15 h) were evaluated with regard to MP numbers. The number of cells with 4 MPs was divided by the number of cells showing 1, 2 or 3 MPs in Cdc15↓ and control cells. The graph displays medians of five biological replicates ± S.E.M. (** = $p \leq 0.01$; Wilcoxon-Mann-Whitney test).

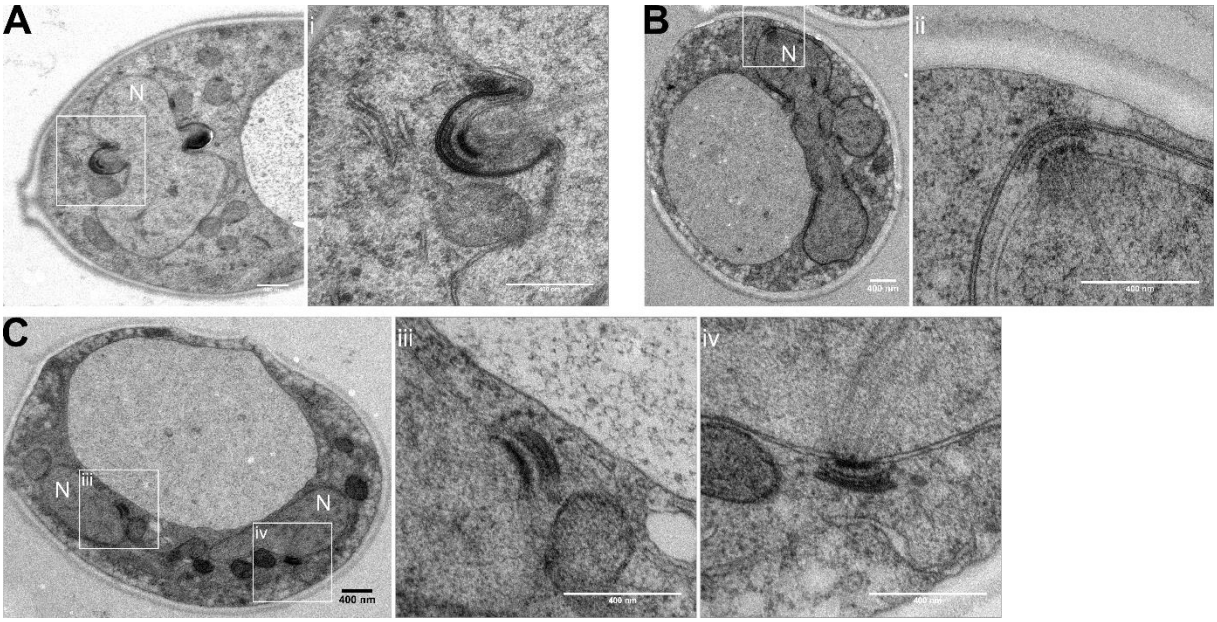

Figure S9 – Meiotic plaques in the Cdc15↓ and Dbf2↓ Dbf20↓ Mob1↓ mutants show no morphological changes.

Electron microscopy (EM) analysis of MP morphology in a control strain (YCR536), a Cdc15↓ strain (YCR688), and a Dbf2↓ Dbf20↓ Mob1↓ strain (YCR539) sporulated in 1 % potassium acetate. Location of nuclei (N) are indicated in the images. Samples of sporulating cells were collected at 6 h after transfer to liquid 1 % acetate medium and processed for EM analysis. A) Overview of a control cell and close up an SPB with MP at an early stage of PSM formation (i). B) Same as **A** in a Cdc15↓ strain at an intermediate stage of PSM formation (ii). C) Overview and close up of two SPBs with MP in a Dbf2↓ Dbf20↓ Mob1↓ strain at the onset of PSM formation (iii and iv). Scale bars: 400 nm.

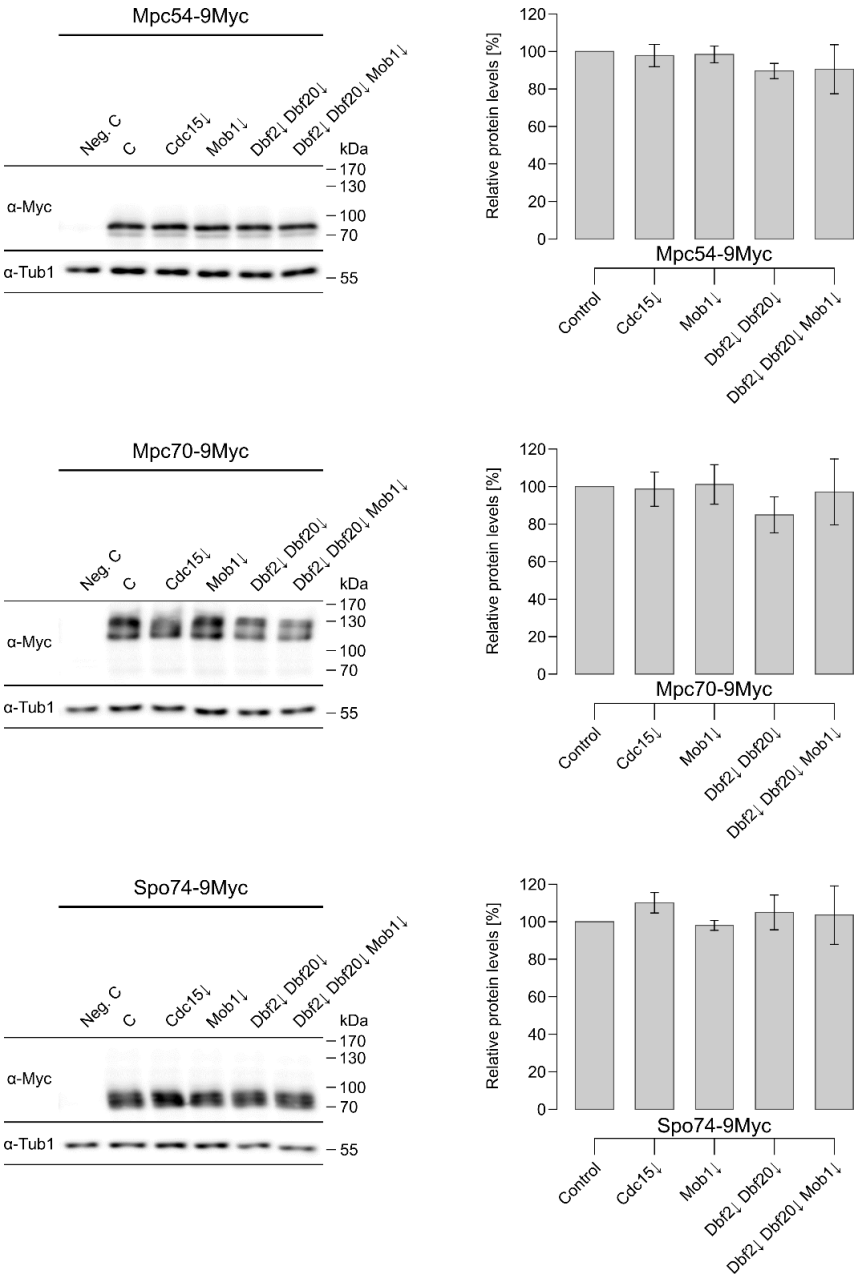

Figure S10 – Meiotic plaque protein levels in the Cdc15↓, Mob1↓, Dbf2↓ Dbf20↓ and Dbf2↓ Dbf20↓ Mob1↓ mutants. *MPC54*, *MPC70* and *SPO74* were endogenously tagged with *9Myc* in the Cdc15↓ (YCR541; YCR546; YCR551, respectively), Mob1↓ (YCR540; YCR547; YCR552, respectively), the Dbf2↓ Dbf20↓ (YCR543; YCR548; YCR553, respectively), the Dbf2↓ Dbf20↓ Mob1↓ (YCR544; YCR549; YCR554, respectively) and in a control strain (C; YCR540; YCR545; YCR550, respectively). Strains were then subjected to sporulation in liquid medium (1 % acetate) and samples were taken every hour from 5 h to 10 h after induction of sporulation. Western blot analysis was performed with pooled samples. A strain without modifications was used as negative control (neg. C; YCR329). Meiotic plaque proteins were detected using anti-Myc antibody and signals of an anti-Tub1 antibody served as loading control. The left panel shows the Western blot signals, the right panel quantifications of protein amounts corrected for Tub1 and normalized to the control (means of four biological replicates ± S.E.M.).

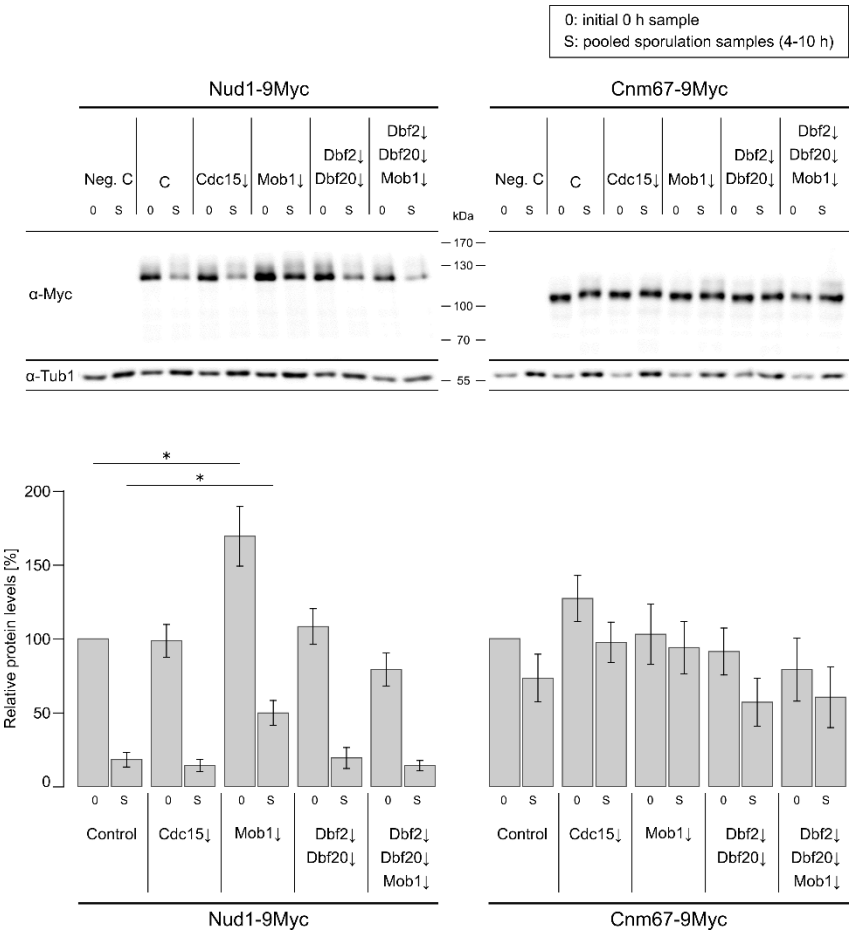

Figure S11 – Levels of the SPB outer plaque proteins Nud1 and Cnm67 during sporulation in Cdc15↓, Mob1↓, Dbf2↓ Dbf20↓ and Dbf2↓ Dbf20↓ Mob1↓ strains. The SPB protein Nud1 and in parallel Cnm67 were fused to 9Myc in the indicated depletion mutants (Nud1: Cdc15↓: YCR608; Mob1↓: YCR609; Dbf2↓ Dbf20↓: YCR610; Dbf2↓ Dbf20↓ Mob1↓: YCR611; Cnm67: Cdc15↓: YCR614; Mob1↓: YCR615; Dbf2↓ Dbf20↓: YCR616; Dbf2↓ Dbf20↓ Mob1↓: YCR617) and a control with only P_{IME2}-*pTEV*$^{+}$-T_{DIT1} (C; YCR607; YCR613, respectively). A strain without 9Myc tag served as negative control (YCR329). Strains were sporulated in liquid 1 % acetate and samples were collected at 0 h as well as every hour from 4 h to 10 h. The initial sample and pooled 4-10 h samples were subjected to immunoblotting. Anti-Myc antibody was used for detection of Nud1-9Myc and Cnm67-9Myc, respectively, anti-Tub1 antibody served as loading control. The upper panel shows the immunoblot signals; for the graphs in the lower panel, signals were quantified, corrected for Tub1 and normalized to the 0 h control values. Bars represent the means of at least three biological replicates ± S.E.M., statistical significances of differences to the control were checked by either one-sample t-tests against 100 % for 0 h values or two-sample t-tests against control for values from pooled sporulation samples (∗: $p \leq 0.05$).

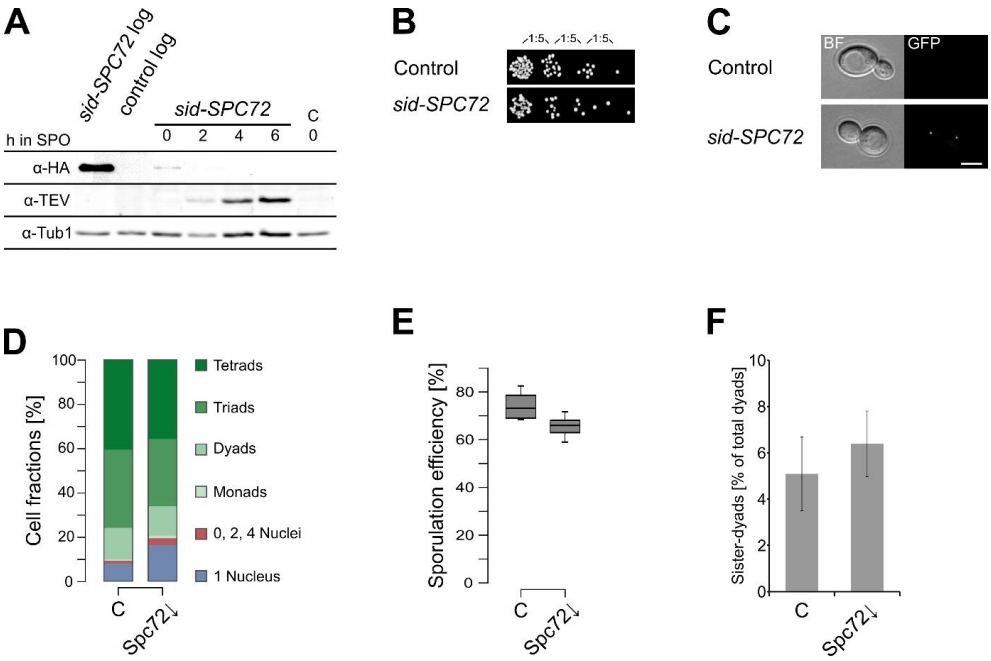

Figure S12 – Sporulation-specific protein depletion, vegetative characterization, and sporulation analysis of a *sid-SPC72* strain.

A – Sporulation-induced depletion of sid-Spc72. A depletion mutant of Spc72 (YDS328) was sporulated together with a control strain (C; YAA146) in liquid 1 % potassium acetate. Samples were collected at the indicated time points. The fusion proteins were detected by anti-HA antibody, pTEV$^+$ production was followed with anti-TEV antibody.Tub1 was used as loading control.

B – Vegetative growth of the *sid-SPC72* strains. Serial 1:5 dilutions of the strains of **A** were spotted in on solid YPD medium and images were taken after 2 days at 30 °C.

C – Mitotic localization of sid-Spc72. The same strains as in **A** were grown to mid-log phase in LFM + 2 % glucose and images in brightfield (BF) and GFP channels were taken. Scale bar: 2 µm.

D – Sporulation profiles of the Spc72↓ strain. The Spc72↓ (YDS328) and the control (C; YAA146) strains were sporulated on solid medium with 1 % acetate. Cells were counted according to cell morphology and number of nuclei. Means of at least 4 biological replicates are shown (156 – 220 cells per replicate). Please see Table S1 for statistical evaluations.

E – Sporulation efficiency of the Spc72↓ strain. Sporulation efficiencies were calculated from the sporulation profile shown in **D**. No statistical significant differences to the control were found in Wilcoxon-Mann-Whitney tests ($n \geq 4$; $p \geq 0.05$).

F – Sister dyad formation is not affected by Spc72-depletion. The experiment was performed with a Spc72↓ (YDS425) and a control strain (YCR481) as described for **Figure 3B**. Dyads with one spore of each color (non-sister dyads) and with both spores containing the same fluorophore (sister-dyads) were counted. No statistically significant differences to the control were found (Wilcoxon-Mann-Whitney; error bars: S.D.; n = 2 for control, n = 4 for Spc72↓; 123 – 227 cells were evaluated for each replicate).

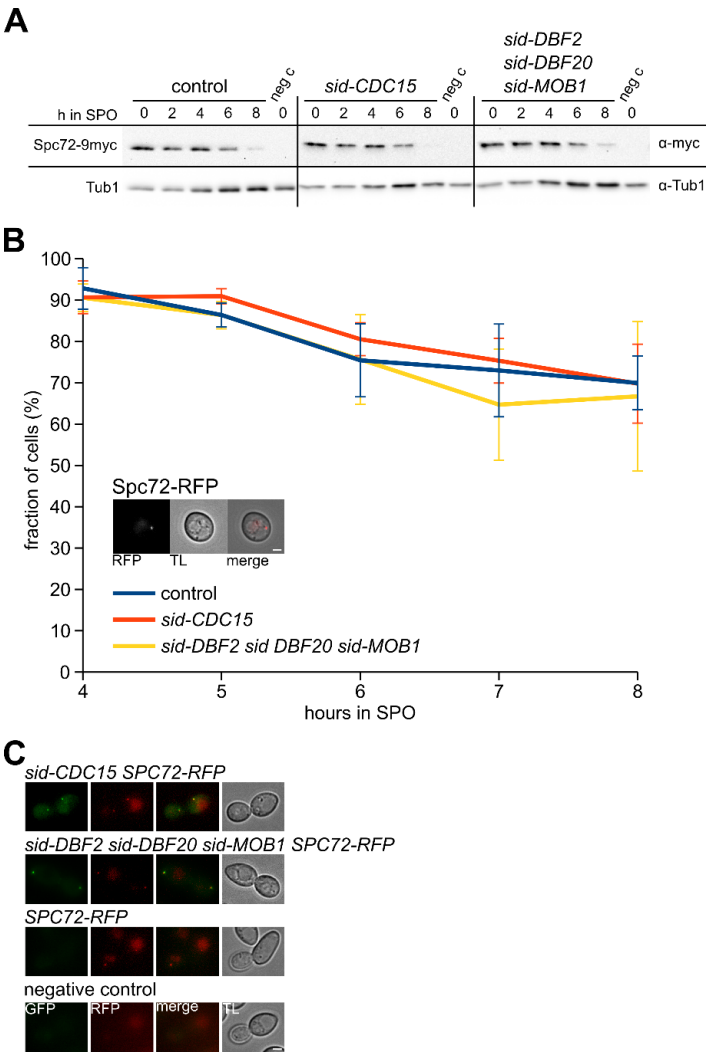

Figure S13 – Spc72 levels and localization during sporulation.

A – Reduction of Spc72 levels during meiosis. Control (YDS419) and MEN mutant strains (Cdc15↓: YDS418; Dbf2↓ Dbf20↓ Mob1↓: YDS420) with Spc72-9myc were sporulated in liquid medium (1 % potassium acetate). Samples were taken at the indicated time points and subjected to Western blotting. A strain without Spc72-9myc was used as negative control (neg c; YCR329). Spc72 was detected using anti-Myc antibody; signals of an anti-Tub1 antibody served as loading control.

B – The number of cells with Spc72 signal at SPBs decreases over time after induction of sporulation. Time course analysis of Spc72-RFP behavior in a Cdc15↓ (YDS416), a Dbf2↓ Dbf20↓ Mob1↓ (YDS427), and a control strain (YDS417) under high acetate conditions (4 – 8 h). Fraction of cells with single-dot Spc72-RFP signal are shown. Four biological replicates were performed (error bars: S.D.; 200 – 300 cells were evaluated for each time point and each replicate; scale bar: 5 µm).

C – Colocalization analysis of Spc72-RFP with sid-tagged MEN components during vegetative growth. Cultures of the same strains as in **B** were grown to mid-log phase in LFM with 2 % glucose and images were taken in brightfield (BF), GFP, and RFP channels. Maximum projections of z-stacks are shown. A strain without Spc72-RFP (YCR329) was used as negative control. Scale bar: 5 µm.

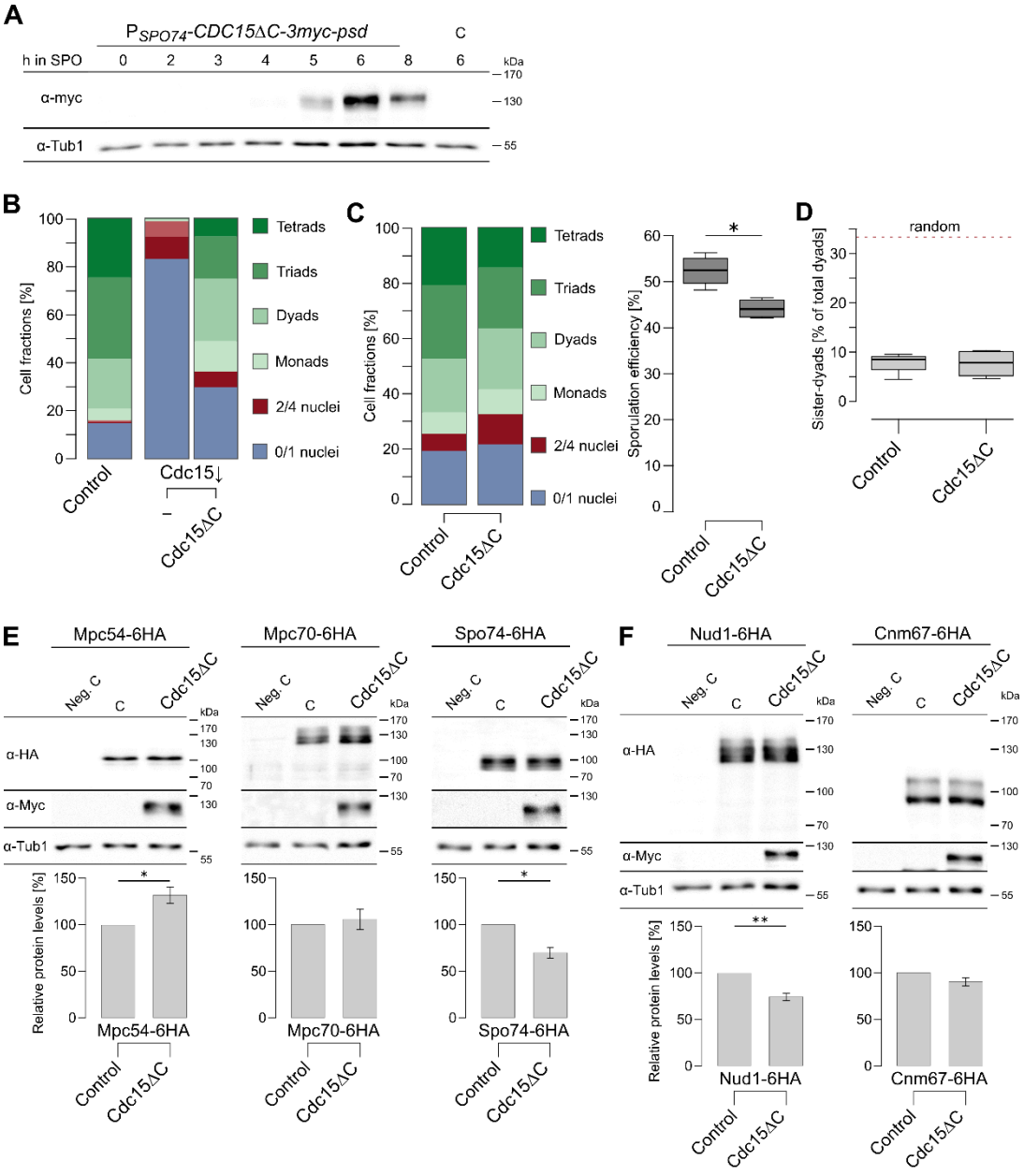

Figure S14 – Hyperactivation of Cdc15 interferes with spore formation and changes in protein levels of Nud1 and meiotic plaque components.

A – Sporulation-specific production of Cdc15ΔC-3myc-psd. A strain (YCR370) with plasmid-borne *CDC15ΔC-3myc-psd* under control of the *SPO74* promoter (pCR118) or an empty vector (C; pRS315) was subjected to sporulation in liquid 1 % acetate and darkness. Samples were collected at the indicated time points. The Cdc15-3myc-psd construct was detected using anti-Myc antibody, anti-Tub1 antibody served as loading control.

B – Complementation of the Cdc15↓ phenotype with Cdc15ΔC. A Cdc15↓ (YCR575) strain transformed with either an empty vector (–; pRS315) or a plasmid with the P*SPO74*-*CDC15ΔC-3myc-psd* construct (Cdc15ΔC; pCR118) was subjected to sporulation on solid medium with 1 % acetate. A control strain (C; YAA146) with an empty vector (pRS315) was used as reference for wild-type sporulation. Cells were counted according to their morphology and number of nuclei. The plot shows means

of at least four biological replicates, between 151 and 588 cells were counted per replicate. Please see Table S1 for statistical evaluations.

C – Meiosis-specific production of Cdc15ΔC results in slightly reduced spore numbers. Sporulation of a diploid strain (YCR370) transformed with either an empty vector (Control; pRS315) or a plasmid bearing a truncated *CDC15* construct (Cdc15ΔC; codons 1-750; pCR118) under control of the mid-sporulation-specific promoter of *SPO74*. Sporulation was performed as described for **Figure 1D**. Left panel shows the means of the different cell classes, right panel sporulation efficiencies ($n \geq 4$; 192 – 754 cells per replicate; ∗: $p \leq 0.05$ in a Wilcoxon-Mann-Whitney test).

D – Sister-dyad formation in the presence of Cdc15ΔC. Strains as in **A** were sporulated on solid medium with 0.1 % acetate. Heterozygous, spore-autonomous markers CENV::$P_{YKL050C}$-*RFP* and CENV::$P_{YKL050C}$-*GFP* allowed assessment of sister dyad formation. Dyads with one GFP-containing and one RFP-containing spore were counted as non-sister dyads; asci with two spores with identical fluorophores were classified as sister-dyads. Differences in the fraction of sister dyads were found not to be statistical significant (Wilcoxon-Mann-Whitney test; $p \geq 0.05$; $n = 4$; 42 – 302 cells per replicate).

E – Aberrant meiotic plaque protein levels in response to Cdc15ΔC. Strains with the meiotic plaque components Mpc54 (YCR484), Mpc70 (YCR485) and Spo74 (YCR486) tagged with 6HA were transformed with the same plasmids as in **A** and subjected to sporulation in liquid medium (1 % acetate). Samples collected at 4 h, 5 h, 6 h, 7 h, 8 h, 9 h and 10 h post-induction were pooled and subjected to western blot analysis. Anti-HA antibody was used to detect the meiotic plaque proteins; anti-Myc antibody visualized production of the Cdc15ΔC construct, anti-Tub1 antibody served as loading control. Upper panel: Western blot signals. Lower panel: quantified meiotic plaque protein levels corrected for Tub1 and normalized to the respective controls ($n = 4$; means ± S.E.M.; ∗: $p \leq 0.05$ in a one-sample t-test).

F – Nud1 and Cnm67 levels in the presence of Cdc15ΔC during sporulation. Experiment was performed as described in **E** with a *NUD1-6HA* (YCR606) and a *CNM67-6HA* (YCR612) strain. The upper panel shows Western blots, the lower panel shows quantified protein levels of four biological replicates, which were corrected using the loading control Tub1 and normalized to the control. Differences were found not to be statistical significant in an unpaired t-test (mean ± S.E.M.; $p \geq 0.05$).

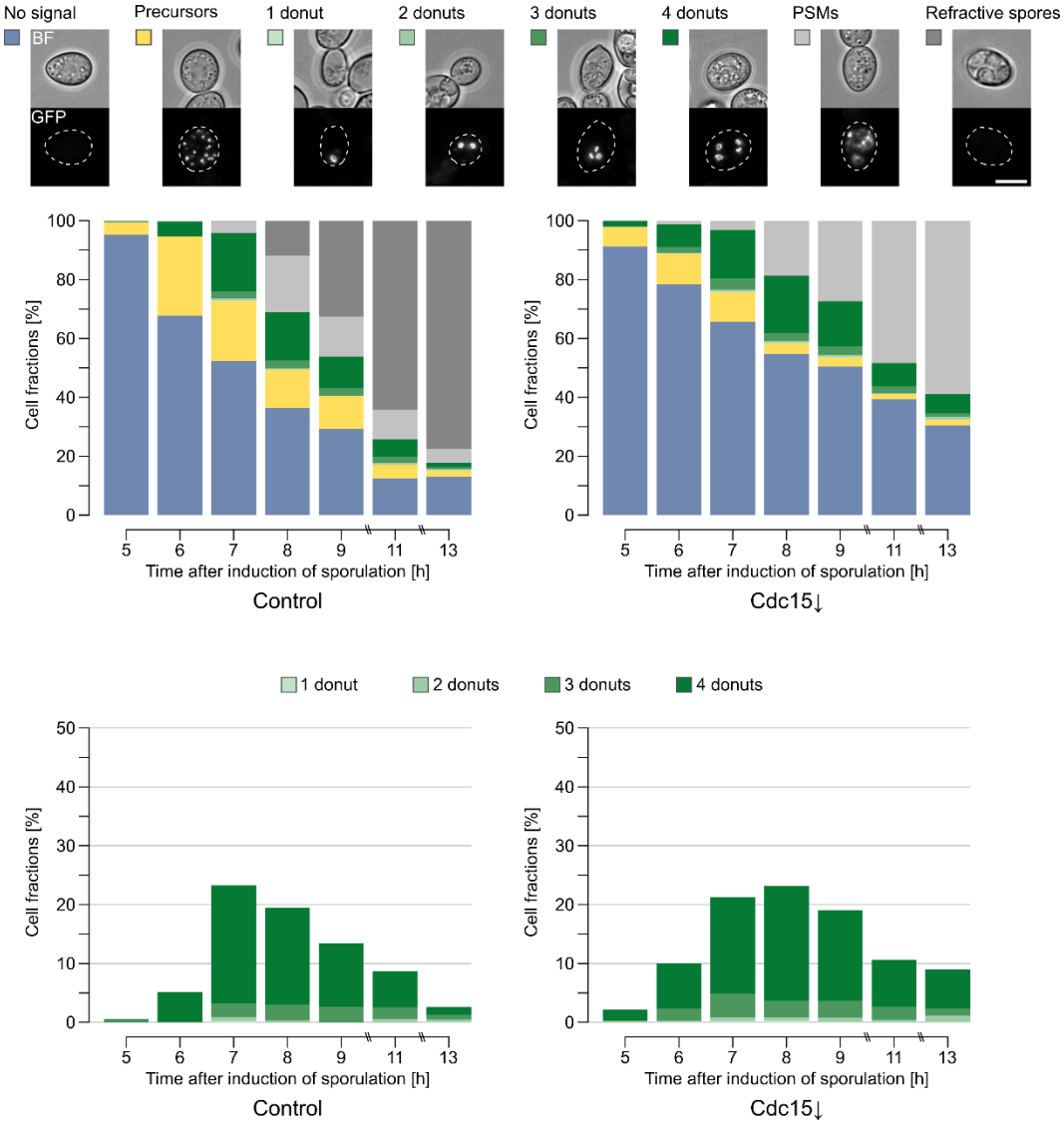

Figure S15 – Defects of the Cdc15↓ mutant in PSM closure and spore maturation. Time course analysis of PSM formation in a Cdc15↓ (YCR332) and a control strain (YCR358) under high acetate conditions (5-13 h). Don1-GFP was used as marker for the leading edge of PSMs. Cell species were distinguished by correlation of fluorescent and brightfield images: prior to meiosis I (no Don1-GFP signals; blue), prior to meiosis II (Don1-GFP at precursor vesicles; yellow), in meiosis II with one to four donuts (Don1-GFP signals at the leading edges of PSMs; light to dark green), cells at/after closure of the PSMs (Don1-GFP signals at whole PSMs; light grey) and cells with refractive spores (dark grey). Upper panel shows fractions of all cell classes, lower panel only cells with donuts (Control: n = 2, Cdc15↓: n = 3; 149 – 499 cells per timepoint and replicate; please see Table S1 for statistical evaluations; scale bar: 5 µm). Please note that in contrast to the control the Cdc15↓ strain bore the *DON1-GFP* fusion only heterozygously, which hindered detection of precursor vesicles.

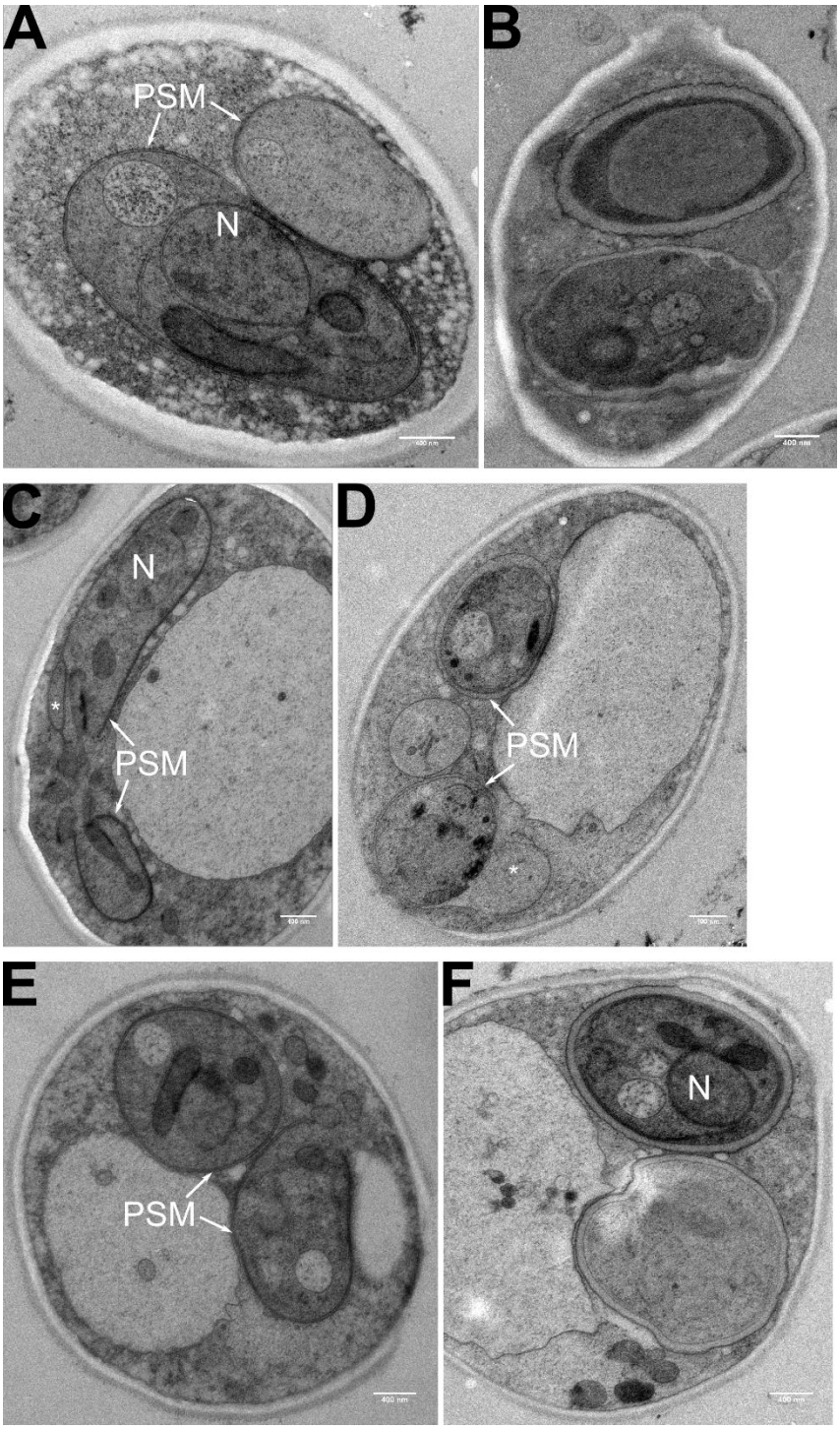

Figure S16 – Unusual PSM morphology in Cdc15↓ cells. Electron microscopy (EM) analysis of a control strain (YCR536), a Dbf2↓ Dbf20↓ Mob1↓ strain (YCR539), and a Cdc15↓ strain (YCR688) under high acetate conditions. Location of nuclei (N) and prospore membranes (PSM) are indicated in the images. Samples of sporulation cells were collected at 9 h after transfer to liquid 1 % acetate medium and processed for EM analysis. **A**) Control cell with prospore prior to PSM closure**. B**) Ascus with spores of control cells. **C**) and **D**) Cdc15↓ cell with abnormal PSM morphology, the asterisk indicates a PSM area with enlarged lumen. **E**) Same as in **A** showing a Dbf2↓ Dbf20↓ Mob1↓ cell. **F**) Same as in **B** showing a Dbf2↓ Dbf20↓ Mob1↓ cell. Scale bars: 400 nm.